AD-A051 825 CALIFORNIA UNIV LOS ANGELES DEPT OF MATERIALS F/G 11/6
A NOTE ON THE ANISOTROPIC ACOUSTIC EMISSION BEHAVIOR OF HSLA ST--ETC(U)
UNCLASSIFIED FEB 78 K ONO, M SHIBATA, M A HAMSTAD N00014-75-C-0419
TR-78-02 NL

| OF |
AD
A051 825

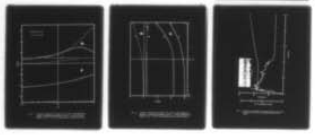

END
DATE
FILMED
4 78
DDC

Technical Report No. 78-02

to the

Office of Naval Research

Contract No. N00014-75-C-0419

A NOTE ON THE ANISOTROPIC ACOUSTIC EMISSION BEHAVIOR OF HSLA STEELS

Kanji Ono and M. Shibata
Materials Department
School of Engineering and Applied Science
University of California
Los Angeles, California 90024

and

M. A. Hamstad
Lawrence Livermore Laboratory
University of California
Livermore, California 94550

February 1978

SECURITY CLASSIFICATION OF THIS PAGE (When Data Entered)

REPORT DOCUMENTATION PAGE

READ INSTRUCTIONS BEFORE COMPLETING FORM

1. REPORT NUMBER: ONR Technical Report No. 78-02
2. GOVT ACCESSION NO.
3. RECIPIENT'S CATALOG NUMBER: (14) TR-78-02

4. TITLE (and Subtitle): (6) A Note on the Anisotropic Acoustic Emission Behavior of HSLA Steels.

5. TYPE OF REPORT & PERIOD COVERED: (9) Technical rept.

6. PERFORMING ORG. REPORT NUMBER

7. AUTHOR(s): (10) Kanji/Ono, M. /Shibata, M. A./Hamstad

8. CONTRACT OR GRANT NUMBER(s): (15) N00014-75-C-0419

9. PERFORMING ORGANIZATION NAME AND ADDRESS
Materials Department - 6531-Boelter Hall
University of California
Los Angeles, CA 90024

10. PROGRAM ELEMENT, PROJECT, TASK AREA & WORK UNIT NUMBERS

11. CONTROLLING OFFICE NAME AND ADDRESS
Physics Program
ONR - 800 N. Quincy Street
Arlington, VA 22217

12. REPORT DATE: (11) Febr[illegible]978

13. NUMBER OF PAGES: 13 (12) 15p.

14. MONITORING AGENCY NAME & ADDRESS (if different from Controlling Office)

15. SECURITY CLASS. (of this report): Unclassified

15a. DECLASSIFICATION/DOWNGRADING SCHEDULE

16. DISTRIBUTION STATEMENT (of this Report)

Unlimited

17. DISTRIBUTION STATEMENT (of the abstract entered in Block 20, if different from Report)

18. SUPPLEMENTARY NOTES

19. KEY WORDS (Continue on reverse side if necessary and identify by block number)

Acoustic Emission
Steel
Inclusion
Internal Stress

20. ABSTRACT (Continue on reverse side if necessary and identify by block number)

Elongated MnS inclusions in HSLA steel produces no detectable burst emission activity when a steel test sample is stressed in tension or in compression along the longitudinal direction. This is in sharp contrast to significant burst emission activities when the tensile stress acts normal to the flattened MnS inclusions in the thickness direction samples of the same HSLA steel. The experimental results are consistent with calculations of internal stresses in and around an oblate inclusion.

DD FORM 1 JAN 73 1473 EDITION OF 1 NOV 65 IS OBSOLETE
S/N 0102 LF 014 6601

SECURITY CLASSIFICATION OF THIS PAGE (When Data Entered)

406 237

TC

A NOTE ON THE ANISOTROPIC ACOUSTIC EMISSION BEHAVIOR OF HSLA STEELS

In recent years, acoustic emission (AE) has become one of the viable nondestructive evaluation methods. It is especially suited for locating flaws in large pressure vessels and elaborate AE testing facilities have been developed and deployed[1]. Numerous laboratory studies have been conducted in order to understand the origins of AE. Results in many studies are inconclusive because of the lack or difficulties in establishing physical processes that produce AE signals.

AE characteristics of a material sometimes exhibit substantial dependence on the loading direction with respect to the direction of prior mechanical working, such as rolling and forging. Graham[2] made the first systematic observation of this effect on a number of structural alloys including 2024, 2219, 2048, 7075, and 6061 aluminum alloys and A533B and HY80 steels. He reported that total AE events normalized by total plastic strain during a tensile test is 1.5 to 32 times higher in a sample oriented along the thickness direction than that along the rolling direction. In the Graham study, effects of continuous-type AE signals were negligible because of the low sensitivity of the transducer, small gage volume of the specimen and relatively low strain rate employed. Hamstad et al.[3] showed that continuous-type AE signals from tensile or compressive testing of 2124 aluminum alloy also exhibit substantial anisotropy. In the thickness direction, the rms peak intensity level was about twice that in the longitudinal or transverse direction.

Noting the significant directional mechanical properties of hot-rolled steels, Ono and coworker[4,5] examined AE characteristics of HSLA steels in the rolling or longitudinal (L), transverse (T) and thickness or short

transverse (Z) directions. The steels tested were of JIS Type SM50 steel with the nominal composition of 0.15% C, 1.30% Mn, 0.35% Si, 0.02% P, and 0.04% Aℓ. The sulphur content was varied from 0.006% to 0.027%. Tensile tests were performed on as-rolled materials having ferrite plus pearlite microstructures.

The main results of the study were as follows: (1) Samples in the L or T direction produced significant AE activities only during initial yielding, consisting primarily of continuous-type AE with a few burst emissions. The level of AE activity was independent of the sulphur content. (2) AE from samples in the Z direction was predominantly of burst-type, and was observed from the pre-yield region to the maximum load. The total AE event counts and the rms peak intensity levels increased with the sulphur content.

Burst-type AE signals in the Z direction samples were interpreted to originate from the decohesion or fracture of MnS inclusions because of the observed directionality and sulphur dependence. Fractographic observations supported this interpretation, which was also consistent with increases in the density of stringer-type inclusions with the sulphur content[6,7].

Evidently, stress concentrations at the inclusions are responsible for the observed behavior and need to be evaluated quantitatively. Eshelby theory of transformation induced stresses[8] has been employed successfully to obtain internal stresses in and around an ellipsoidal inclusion[9,10]. Recently, Shibata and Ono[11,12] considered internal stresses in an oblate spheroidal inclusion and at the inclusion-matrix boundary arising from the following three effects; namely, (1) misfit effect due to a difference in thermal expansion coefficients of the inclusion and matrix, (2) inhomogeneity effect due to a difference in the elastic stiffnesses of the inclusion and matrix and (3) plastic deformation effect due to the presence of a non-

deformable inclusion in the matrix, which is plastically deformed. For the latter two effects, the oblate spheroidal inclusion had its broad face either normal (N configuration) or parallel (P configuration) to the direction of external stress and plastic deformation. Their results are adopted to consider an MnS inclusion in steel. The inclusion is approximated by a disc even though a typical MnS inclusion in hot rolled steel has the shape of a ribbon[6,7]. Thus an inclusion of N configuration represents one in the Z direction sample, whereas that of P configuration approximates an MnS inclusion in the L or T direction samples. The thickness-to-diameter ratio, k, is expected to be 0.01 to 0.1. It is assumed that the steel matrix ceases to allow plastic relaxation around the inclusion below 800 K, giving rise to thermal misfit strain, ε^T, of -3×10^{-3}. The ratio of Young's moduli of MnS and steel, m, is found to be 2/3[11]. The magnitude of uniaxially applied stress, σ^A, is taken at 10^{-3}E or 206 MPa, where E is the Young's moduli of steel. This stress level is approximately 60% of the yield strength, above which burst emission activities become significant[4,5]. The amount of plastic deformation of the matrix, ε_p, is taken as 1%, as lower values of ε_p produce insignificant effects on the total internal stress.

Two components of internal stress, normal to the board face of the inclusion, were calculated for inclusions of N and P configurations under either tensile or compressive loading. Results are presented in Figs. 1 and 2, where the normal stresses, σ, are expresses in terms of E and plotted against k. Here, A refers to a point on the equator of the inclusion and B to the polar points. At A, σ actually corresponds to tangential stress acting at the interface (σ^M_{33} for N configuration in Ref. 11 and σ^M_{11} in P configuration in Ref. 12). At B, σ refers to normal stress acting at the interface, which is equal in magnitude to the corresponding stress within the inclusion (σ^I_{33} for N configuration in Ref. 11 and σ^I_{11} for P configuration in Ref. 12).

Under tensile loading, Fig. 1 shows that an MnS inclusion of N configuration is subjected to tensile stresses at A and B. The inhomogeneity effect is the primary element for σ at B for N configuration, $\sigma(N,B)$, especially for smaller values of k. As k increases, the misfit effect becomes significant and accounts for much of stress intensification at $k \simeq 0.1$. The plastic deformation effect is an important part of $\sigma(N,A)$, since the misfit effect produces a large compressive stress in the matrix[10]. In fact, at ε_p less than 0.65 to 0.8%, $\sigma(N,A)$ remains compressive. $\sigma(N,A)$ is, however, sensitive to ε_p and exceeds the normal stress at B for ε_p greater than 1% or so. Thus, decohesion at the edge of the inclusion of N configuration is expected under tensile loading at larger values of ε_p. Initially, the broad face is the favored site, but the inclusion edge becomes the likely site for decohesion with increasing plastic deformation. An inclusion of P configuration is subjected to weakly tensile stress at B, but strongly compressive stress develops at A. Consequently, it is unlikely to initiate decohesion for this configuration under tensile loading.

Under compressive loading, σ is mostly compressive with the exception of $\sigma(P,B)$, as shown in Fig. 2. However, $\sigma(P,B)$ is still smaller than σ^A for $k < 0.1$, and decreases to $\sigma^A/10$ at $k = 0.01$. Since the compressive stresses at A are quite high, the decohesion of the inclusion of either configuration appears to be remote.

The results for tensile loading are consistent with the previous interpretation of the observed AE behavior of HSLA steel[5]. The calculation indicates that a stress of 200 to 300 MPa initiates the decohesions at the face of the MnS-steel interface for N configuration. As the decohesion may initiate from both face on opposite sides of an inclusion, fracture perpendicular to the inclusion face necessarily accompanies the process. The

inherent fracture strength of MnS is expected to be much higher than the indicated decohesion strength so that internal fracture of MnS parallel to the broad face appears unlikely. It is also interesting to note that another normal stress along the tensile axis within the inclusion of P configuration is quite high. This component is σ^I_{33} in Ref. 12 and, for k of 0.01 to 0.1,

$$\sigma^I_{33} \simeq 2.35\ \sigma^A + 0.85\ m\ E\varepsilon_p\ .$$

From this, at ε_p = 1%, σ^I_{33} becomes 1.7 GPa taking $\sigma^A = 10^{-3}$ E. This high tensile stress may incur fracture of the inclusion. Because of the matrix constraint and a limited volume of strain energy relaxation, an AE signal from such a fracture event appears to be too weak to be detected.

Under compressive loading, normal tensile stress components within the inclusion perpendicular to σ_A become significant. For N configuration, these are σ^I_{11} and σ^I_{22} in Ref. 11 and reach 1.1 GPa under the same condition as above. For P configuration, it corresponds to σ^I_{22} in Ref. 12 and amounts to 0.7 GPa. Again, no detectable AE activity is expected from these loading conditions.

During compression tests, several investigators[13,14] have reported vastly decreased AE activities in a number of structural materials. However, compression testing of HSLA steels with aligned MnS inclusions has not been monitored via AE techniques. In order to correlate the present results with careful monitoring of waveform of AE signals, compression samples of square cross section (12.4 mm x 12.4 mm x 31.8 mm) were machined from two hot rolled plates along the L direction. The two plates were from a single slab of JIS SM-50 steel with the chemical analysis of 0.17% C, 1.29% Mn, 0.34% Si, 0.019% S, 0.016% P, 0.029% Aℓ. The average size and density of MnS inclusions on

the LZ plane as determined by standard metallographic technique were 60 μm and 5 to 8 x $10^3/cm^2$, respectively.

Test procedures were described in detail elsewhere[3]. The transducer, which was attached to the side of a sample, was of resonant-type (Model C 175 B, AET Corp., Sacramento, Calif.). The filter bandwidth was 100 to 300 kHz. The rms voltages were recorded along the load and displacement. The latter was obtained by using a clip gage with 12.7 mm gauge length. Waveform of the AE signals was monitored on an oscilloscope during a test and using a transient recorder from tape recording after a test. A universal testing machine (Tinius Olsen Model 60K, 4 screw Electromatic UTM) was employed for the tests at a cross head speed of 4.23 x 10^{-6} m/s. Nominal strain rate was 1.33 x 10^{-4} s^{-1}.

Representative results of stress and rms voltages against strain during a compression test is shown in Fig. 3. The main features of the results are identical to the corresponding tensile tests of the same materials. No evidence of burst-type AE was obtained prior to the yield point or beyond. Main AE activities were observed only during the Lüders elongation. This result is consistent with the calculation which predicts no decohesion for MnS inclusions in the P configuration loaded in compression. A typical waveform at 0.5% strain is given as an insert in Fig. 3 and shows the continuous nature of AE signals.

From this observation along with the calculations presented earlier, we conclude that elongated MnS inclusions in HSLA steel produce no detectable burst emission activity when a steel test sample is stressed in tension or in compression along the L (and probably T) direction. This is in sharp contrast to significant burst emission activities when the tensile stress acts normal to the flattened MnS inclusions in the Z direction samples of the same HSLA steel.

ACKNOWLEDGEMENTS

The authors are grateful to Messers. R. Landy and A. E. Brown for experimental assistance, to Messers. C. Ouchi and J. Tanaka, Nippon Kokan K. K., Kawasaki, Japan for supplying the HSLA steel plates used in this study, and to the Office of Naval Research, Physics and Metallurgy Programs and to the U.S. Department of Energy for financial support.

REFERENCES

1. "Monitoring Structural Integrity by Acoustic Emission" ASTM-STP-571, edited by J. C. Spanner and J. W. McElroy, Amer. Soc. for Testing and Materials, Philadelphia, Penn. 1975.
2. L. J. Graham, "Proc. ARPA/AFML Review of Quantitative NDE", AFML-TR-75-212, pp. 631-42, Air Force Wright Aeronautical Lab., Wright-Patterson AFB, Ohio, 1976.
3. M. A. Hamstad, R. Bianchetti and A. K. Mukherjee, Engr. Fracture Mech. 1977, vol. 9, pp. 663-674.
4. K. Ono, H. Hatano and G. Huang, "Proc. 8th World Conf. on Nondestructive Testing" paper No. 3K3, Cannes, France 1975.
5. K. Ono, G. Huang and A. Kawamoto, "Proc. 6th Int. Conf. on Internal Friction and Ultrasonic Attenuation in Solids", Univ. of Tokyo Press, Tokyo, Japan (in press).
6. I. Kozasu and J. Tanaka, "Sulfide Inclusions in Steel" edited by J. J. de Barbadillo and E. Snape, pp. 286-308, Amer. Soc. Metals, Metals Park, Ohio 1975.
7. T. J. Baker, "Sulfide Inclusions in Steel", edited by J. J. de Barbadillo and E. Snape, pp. 135-38, Amer. Soc. Metals, Metals Park, Ohio 1975.
8. J. D. Eshelby, Proc. Roy. Soc., 1957, vol. A 241, p. 376.
9. K. Tanaka and T. Mori, Acta Met. 1970, vol. 18, pp. 931-41.
10. K. Tanaka, T. Mori and T. Nakamura, Trans. Iron and Steel Inst. Japan, 1971, vol. 11, p. 383.
11. M. Shibata and K. Ono, Acta Met. 1978, vol. 26 (in press).

12. M. Shibata and K. Ono, ONR Tech. Rep. No. 5, Univ. of Calif., Los Angeles, Dec. 1977.

13. S. H. Carpenter and F. P. Higgins, Met. Trans., 1977, vol. 8A, pp. 1629-32.

14. M. A. Hamstad and A. K. Mukherjee, UCRL 77502, Lawrence Livermore Lab., Nov. 1975.

FIGURE CAPTIONS

Fig. 1. Internal stresses at A and B for N and P configurations against thickness-to-diameter ratio, k, under tensile stress of $\sigma^A = 10^{-3}E$ (as indicated by the dotted line).

Fig. 2. Internal stresses at A and B for N and P configurations against thickness-to-diameter ratio, k, under compressive stress of $\sigma^A = 10^{-3}E$ (as indicated by the dotted line).

Fig. 3. Stress and rms voltages of AE signals against strain during a compression test of the longitudinal direction steel sample.

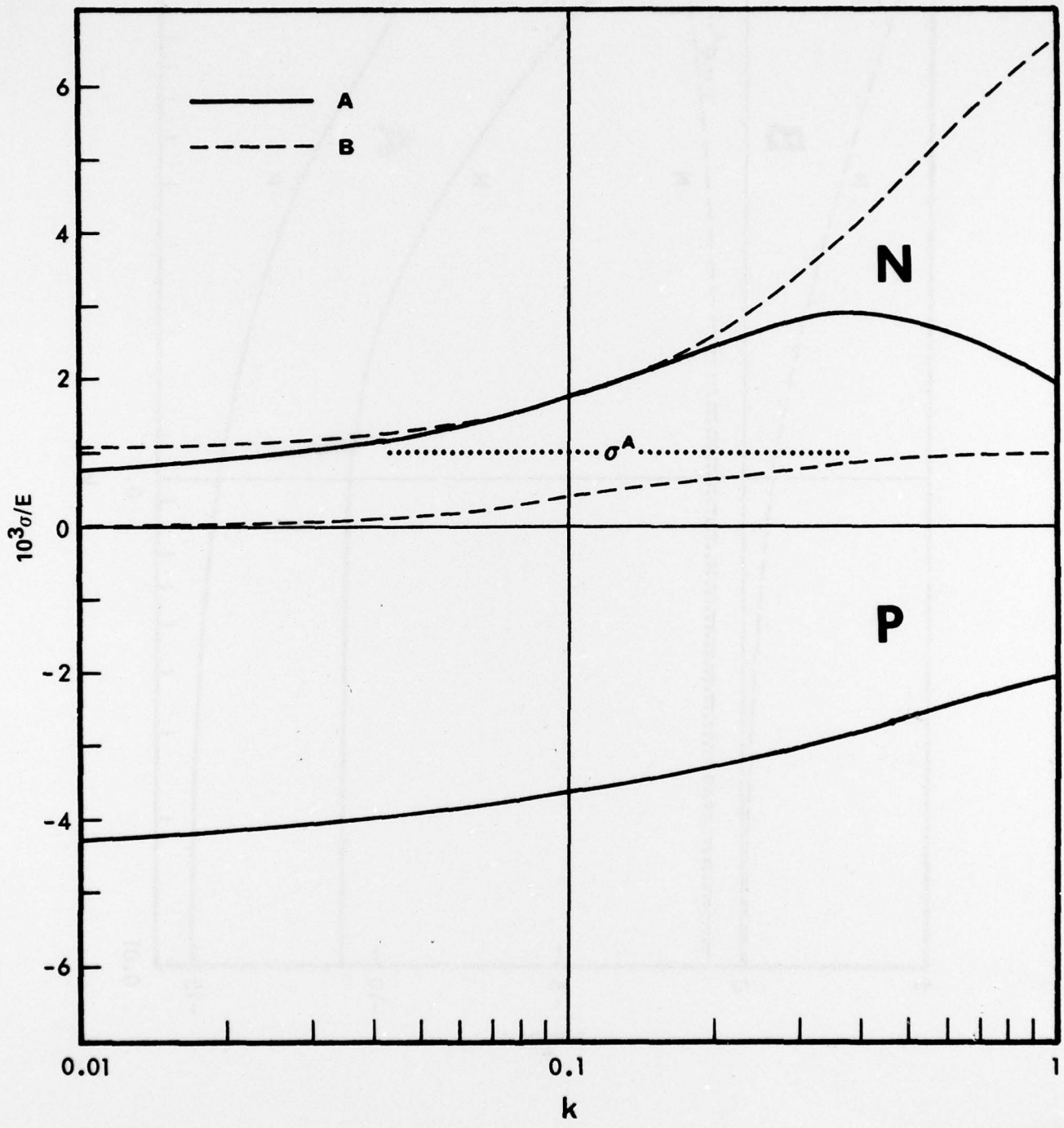

Fig. 1. Internal stresses at A and B for N and P configurations against thickness-to-diameter ratio, k, under tensile stress of $\sigma^A = 10^{-3}E$ (as indicated by the dotted line).

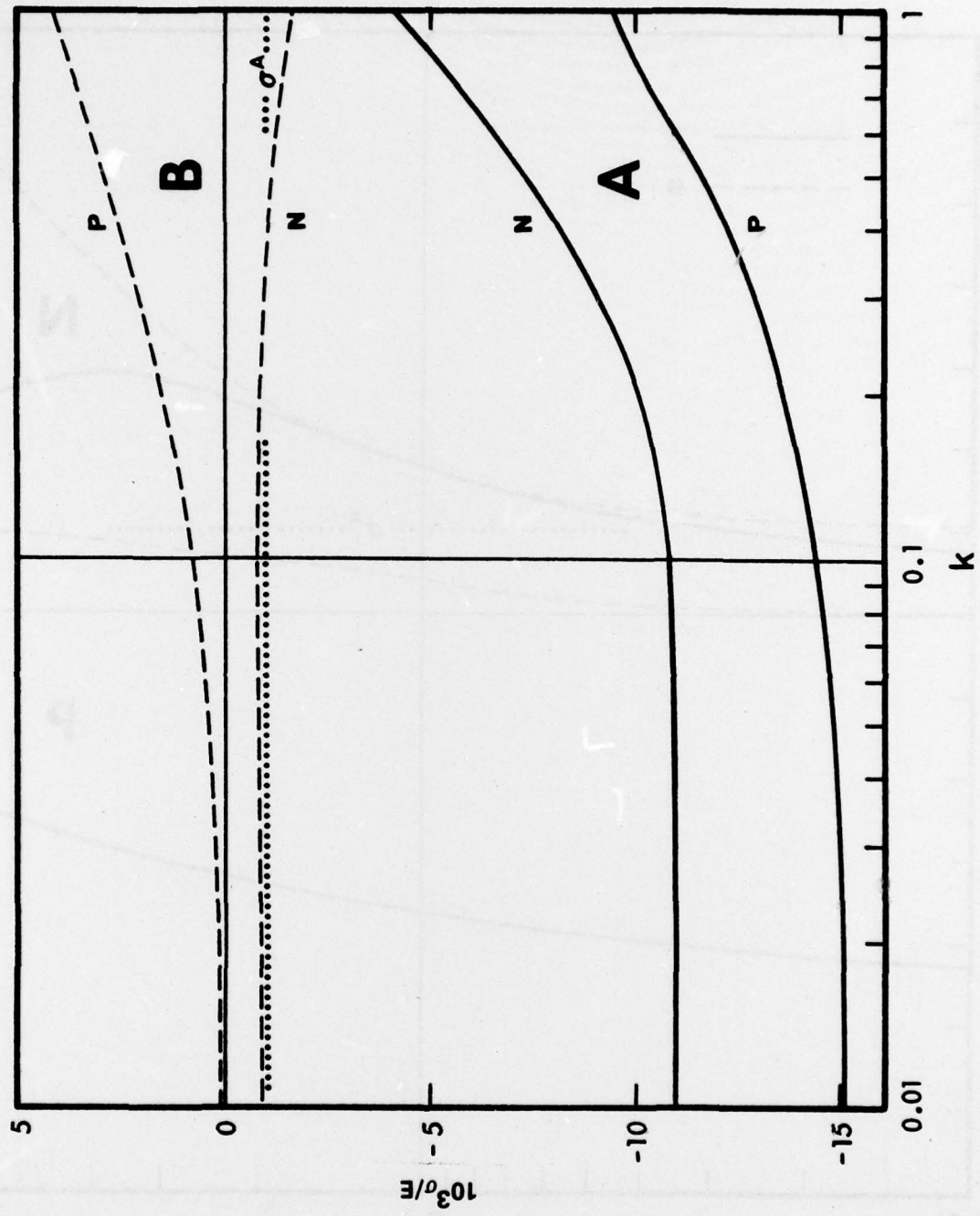

Fig. 2. Internal stresses at A and B for N and P configurations against thickness-to-diameter ratio, k, under compressive stress of $\sigma^A = 10^{-3}E$ (as indicated by the dotted line).

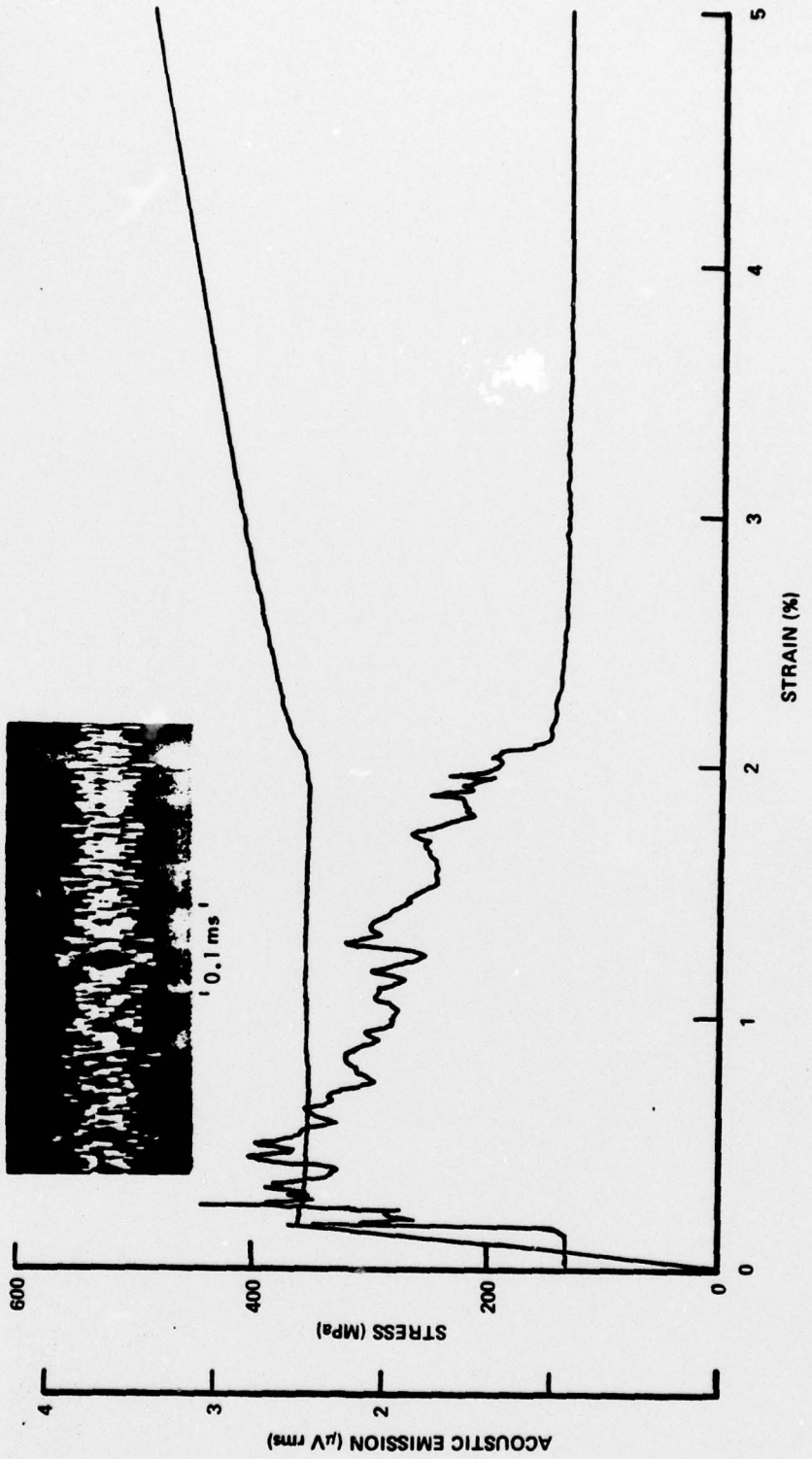

Fig. 3. Stress and rms voltages of AE signals against strain during a compression test of the longitudinal direction steel sample.